

# Octahedral Tilt Instability of $\text{ReO}_3$ -type Crystals

Philip B. Allen

*Department of Physics and Astronomy, State University of New York,  
Stony Brook, NY 11794-3800 (permanent address)*

*and Department of Applied Physics and Applied Mathematics Columbia University, New York, NY 10032*

Yiing-Rei Chen\*

*Department of Physics and Astronomy State University of New York, Stony Brook, NY 11794-3800*

Santanu Chaudhuri† and Clare P. Grey

*Department of Chemistry State University of New York, Stony Brook, NY 11794-3400*

(Dated: December 30, 2021)

The octahedron tilt transitions of  $\text{ABX}_3$  perovskite-structure materials lead to an anti-polar arrangement of dipoles, with the low temperature ( $T$ ) structure having six sublattices polarized along various crystallographic directions. It is shown that an important mechanism driving the transition is long range dipole-dipole forces acting on both displacive and induced parts of the anion dipole. This acts in concert with short range repulsion, allowing a gain of electrostatic (Madelung) energy, both dipole-dipole and charge-charge, because the unit cell shrinks when the hard ionic spheres of the rigid octahedron tilt out of linear alignment.

In 1950 Slater [1] presented an electrostatic theory of the ferroelectric transition in  $\text{BaTiO}_3$  (perovskite  $\text{ABX}_3$  structure) by generalizing the Clausius-Mossotti (CM) picture. An important ingredient is the fact that the local dipolar electric field  $\vec{F}_D$  at the X site differs from the Lorentz value  $(4\pi/3)\vec{P}$  because the local symmetry is less than cubic. Here we present a similar discussion, also highlighting the role of dipole-dipole interactions, of the octahedron tilt commonly found in perovskite structure. To simplify the many interactions, this paper is confined to the  $\text{ReO}_3$  structure type [2] with the perovskite A sublattice empty. We take  $\text{AlF}_3$  as our prototype.

Starting with the parent cubic structure, the ( $R\bar{3}c$  rhombohedral) low  $T$  phase of  $\text{AlF}_3$  is generated by a rigid rotation of an  $\text{AlF}_6$  octahedron through angle  $\omega \approx 0.3\text{rad}$  around a cubic (111) axis through an Al atom. Because neighboring octahedra share corners, rotations alternate, doubling the unit cell according to wavevector  $(\pi, \pi, \pi)$ . A schematic view of the distorted (111) plane is shown in Fig. 1. The Shannon ionic radii [3] of  $\text{Al}^{3+}$  and  $\text{F}^-$  match almost perfectly to an octahedron with the central Al touching the six F anions, and each F anion touching its eight F neighbors. Thus the rigidity of the octahedron follows both from Al-F covalency and from ionic size effects. As the octahedra tilt, their spacing shrinks, generating a rhombic primitive cell whose  $c/a$  ratio increases by the factor  $1/\cos(\omega)$  relative to the cubic value, and cell volume  $V$  decreases as  $\Delta V/V = -\sin^2 \omega$ .

CM theory [4, 5] shows that a cubic lattice of polarizable molecules may have a “polarization catastrophe” sig-

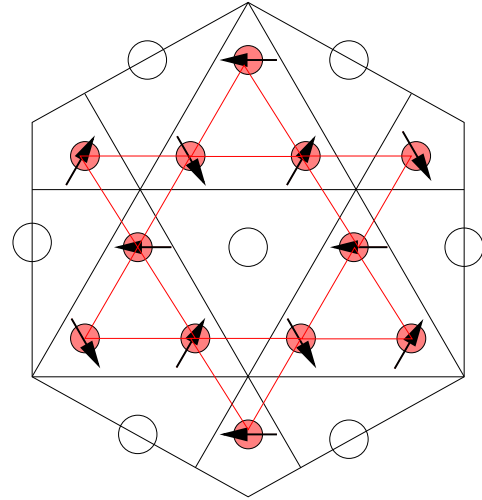


FIG. 1: The (111) planes of perovskite are alternately  $\text{AX}_3$  and B layers. The  $\text{AX}_3$  sites constitute an  $fcc$  lattice with close-packed triangular (111) planes occupied 75% by X anions (shown as filled circles) and 25% by A cations (shown as open circles and missing in the  $\text{AlF}_3$  structure.) Arrows denote displaced X anions. Faint triangles with counter-clockwise rotations have their nearest B cation in the plane below, and inverted faint triangles with clockwise rotations have their nearest B cation in the plane above.

nalling an instability towards ferroelectric polarization. The condition for instability is an increase of the product  $n\alpha$  (density times polarizability) to  $3/4\pi$ . A generalized version of this statement is derived in the Appendix: a self-stabilized spontaneously electrically polarized state will occur when  $\alpha$  increases to  $1/\gamma_{\text{max}}$  where  $\gamma_{\text{max}}$  is the maximum eigenvalue of the dipole-dipole interaction tensor  $\Gamma$ . The tensor  $\Gamma_{i\alpha,j\beta}$  is defined as the  $\alpha$  Cartesian component of the dipolar electric field  $\vec{F}_{D,i}$  (at site

\*current address: Dept. of Chemistry, Columbia University, New York, NY 10032

†current address: Dept. of Chemistry, Brookhaven National Laboratory, Upton, NY 11973

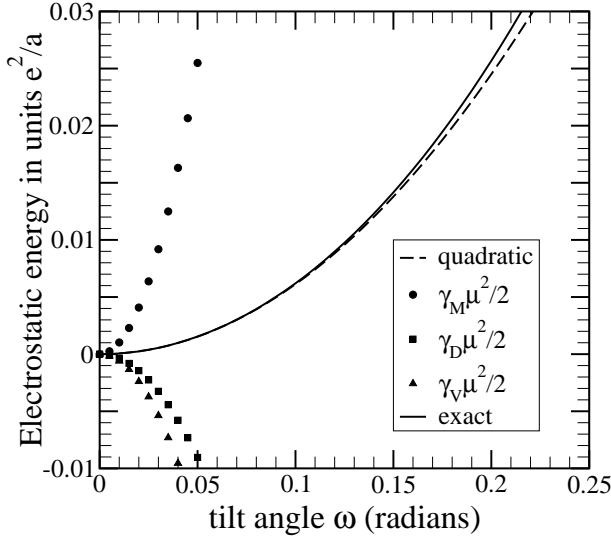


FIG. 2: Electrostatic energy of  $\text{BX}_3$  with full ionic charges  $+3$  and  $-1$ , as a function of the tilt angle  $\omega$  around the  $(111)$  axis. The dashed curve is the full quadratic approximation, namely the sum of the Madelung ( $M$ ), dipole-dipole ( $D$ ), and volume ( $V$ ) terms. The solid curve is the exact Madelung sum.

$\vec{R}_i$  of the lattice) created by a unit dipole in the Cartesian  $\beta$  direction at site  $\vec{R}_j$ . In a  $3 - N$ -vector notation,  $|F_D\rangle = \Gamma|\mu\rangle$ . This generalization of Clausius-Mossotti theory requires no restrictions on the size or symmetry of the system. The pattern of spontaneous polarization, given by the corresponding eigenvector, is in general not a simple ferroelectric.

Rigid rotations of octahedra almost always occur in the low- $T$  phases of perovskites [6, 7].  $\text{AlF}_3$  has the perovskite structure with the A sublattice empty. Below 730K the structure is rhombohedral because of cooperative rotation of  $\text{AlF}_6$  octahedra, as shown in Fig. 1. We have successfully modelled this instability in two different ways: (1) using density-functional theory (DFT) [8], and (2) using classical molecular dynamics (MD) [9], including both short-range and electrostatic forces, plus anion polarizability. In this paper we abstract from our earlier results a simple picture that includes electrostatic effects of charged and polarizable point ions.

The dipole patterns  $|\mu\rangle$  ( $\langle i\alpha|\mu\rangle$  is the  $\alpha$  Cartesian component of the dipole  $\vec{\mu}_i$  on the  $i$ 'th ion) are particularly simple and illuminating. First define the “displacive dipole”  $\vec{\mu}_{D,i}$  of the  $i$ th X anion as  $\vec{\mu}_{D,i} = -\beta e \vec{u}_i$  where  $\vec{u}_i$  is the small displacement from the site  $\vec{R}_i$  of cubic symmetry, and  $-\beta e$  is the charge of the anion. The unknown dimensionless parameter  $\beta$  absorbs the uncertainty about what actual charge to assign. The dipole can be imagined as a separated pair of opposite charges, the negative end at the anion nuclear coordinate  $\vec{R}_i + \vec{u}_i$ , and the positive end at the lattice site  $\vec{R}_i$  formerly occupied by the anion.

Consider the dipole patterns generated by different types of octahedron tilts. In Glazer’s [6] notation, when

the tilt angle is small, any tilt  $\phi^p\psi^q\theta^r$  is a product of tilts around  $\hat{x}$ ,  $\hat{y}$ , and  $\hat{z}$  where  $p, q, r$  are  $+$  or  $-$ . There are six primitive rotations. For example, a  $\hat{z}$ -tilt by angle  $\theta$  is denoted as  $\phi^0\psi^0\theta^\pm$ , where  $p = q = 0$  indicates no rotation around  $\hat{x}$  or  $\hat{y}$ . This tilt belongs to wavevector  $\vec{k} = (\pi, \pi, k_z)$ . Rotations of adjacent octahedra in the  $\hat{x}$  and  $\hat{y}$  directions are forced to be opposite in sign (wavevector  $k_x = k_y = \pi$ ), whereas in the  $\hat{z}$ -direction, the next octahedron can have a different rotation angle. Glazer’s conventions are that  $r = +$  corresponds to  $k_z = 0$ , while  $r = -$  indicates  $k_z = \pi$ . We have discovered the interesting fact, explained in the Appendix, that the corresponding dipole patterns  $|\mu\rangle$  for the six primitive rotations are eigenvectors of  $\Gamma$ . The three  $|\mu(\phi^0\psi^0\theta^+)\rangle$  are degenerate with eigenvalue  $\gamma(+)=14.383/a^3$ , while the three  $|\mu(\phi^0\psi^0\theta^-)\rangle$  are degenerate with eigenvalue  $\gamma(-)=14.461/a^3$  (where  $a=3.43\text{ \AA}$  in  $\text{AlF}_3$ ). Note that  $\gamma(-)$  is the largest eigenvalue of  $\Gamma$ , and that  $\gamma(+)$  is only 0.5% smaller than  $\gamma(-)$ . It follows that the dipole-dipole interaction energy of an arbitrary tilt-induced dipole pattern  $|\mu(\phi^p\psi^q\theta^r)\rangle = \sum C_\gamma |\gamma\rangle$  is  $-\sum |C_\gamma|^2 \gamma/2$ . Thus an arbitrary Glazer tilt has dipole-dipole interaction energy

$$\begin{aligned} E_D(\phi^p\psi^q\theta^r) &= -\frac{1}{2} \left( \frac{\beta e a}{2} \right)^2 [\gamma(p)\phi^2 + \gamma(q)\psi^2 + \gamma(r)\theta^2] \\ &= -\frac{1}{2} [\gamma(p)\mu_x^2 + \gamma(q)\mu_y^2 + \gamma(r)\mu_z^2] \end{aligned} \quad (1)$$

where  $\mu_x = \beta e a \phi/2$  is the amplitude of the dipole eigenarray arising from the  $\hat{x}$  rotations, etc. When  $p, q, r$  are all negative as in  $\text{AlF}_3$ , the dipole-dipole interaction energy  $E_D = -\gamma_D |\vec{\mu}_D|^2/2$  is as negative as possible ( $\gamma_D = \gamma(-)$  is maximal) for any array of displacive dipoles of fixed magnitude  $|\vec{\mu}_D|$ . For cases when the superscripts contain some  $+$ 's, *i.e.* for different Glazer tilting schemes, the energy is at worst 0.5% smaller than optimum.

So far we have presented an argument showing that tilts of corner-coupled rigid octahedra are strongly stabilized by dipole-dipole interactions. All such tilt systems are “6-sublattice” antiferroelectrics, because each of the six anions of a  $\text{BX}_6$  octahedron defines a separate direction of polarization. Although it is reasonable to characterize all such dipolar-stabilized tilt patterns as antiferroelectric, nevertheless conventional use often [5, 10] (but not always [11]) restricts “antiferroelectric” to cases where an applied external field can switch the state to ferroelectric. Therefore we use the term “anti-polar.”

Now we need a theory for the total energy. From our previous studies [8, 9] it is clear that the displacive dipole  $\mu_D$  must be supplemented by an induced dipole  $\mu_I$  on the polarizable anion. This costs energy  $\mu_I^2/2\alpha$  per dipole, where  $\alpha$  is the anion polarizability. The isolated anion in a field  $\vec{F}$  has a moment  $\alpha\vec{F}$  which minimizes the total energy  $\mu_I^2/2\alpha - \vec{\mu}_I \cdot \vec{F}$ . For the  $\text{F}^-$  anion,  $\alpha$  depends somewhat on its environment, but is in the range [12]  $\sim 0.85 \pm 0.05 \text{ \AA}^3$ . We also need to account for the total change of electrostatic energy when anions move, not

just the cooperative dipole-dipole part. Taylor expanding the Madelung energy  $\Phi$  to second order in displacements, two types of energy appear. (1) There is the intersite or dipole-dipole term already computed which alters the energy bilinearly in the total moment  $\mu_{I,i} + \mu_{D,i}$  of dipoles at different sites  $i$  and  $j$ . (2) There is a “Madelung” field  $\vec{\nabla}_i \Phi$  near  $\vec{R}_i$  caused by the ideal undistorted lattice of other ions. This vanishes by inversion symmetry exactly at  $\vec{R}_i$  and grows linearly  $((\vec{u}_i \cdot \vec{\nabla}_i) \vec{\nabla}_i \Phi / 2)$  with displacement from this site. This gives an energy  $\Gamma_{M\alpha\beta} \mu_{D\alpha} \mu_{D\beta} / 2$ . Uncertainty about actual charges is absorbed into the same factor  $\beta$  which was used in the definition of the displacive dipole  $\mu_D$ . From the Poisson equation  $\nabla^2 \Phi = 0$ , the trace of  $\Gamma_M$  is zero. For cubic  $\text{BX}_3$  with charges  $+3$  for B and  $-1$  for X, we find numerically that  $\Gamma_M$  is diagonal in cube body axes, with elements  $\gamma_M = 40.789/a^3$  in the directions transverse to the B-X-B axis (where rotations actually occur) and an element  $-2\gamma_M$  in the direction parallel. This describes a restoring field  $F_M = -\gamma_M \mu_D$  at the site of the displaced X anion nucleus. This field is larger (by  $-2.8$ ) than the destabilizing dipolar field  $F_D = \gamma_D \mu_D$  previously found from the displacements of the other X anions. This explains why the induced moment ( $\mu_I = \alpha(F_M + F_D)$ ) is opposite to the displacive moments.

The energy of the dipole array generated by a tilt is

$$U_{\text{tot}}(\mu_D, \mu_I) = \frac{1}{2\alpha} \mu_I^2 - \frac{1}{2} \gamma_D (\mu_D + \mu_I)^2 + \frac{1}{2} \gamma_M \mu_D^2 + \gamma_M \mu_D \mu_I - \frac{1}{2} \gamma_V \mu_D^2. \quad (2)$$

The second, third, and fourth terms contain the Taylor expansion of the Madelung energy as described above. The fifth term accounts for destabilizing short-range interactions which have not yet been discussed. The large Madelung electrostatic attraction of ionic crystals tries to shrink the lattice constant as much as possible. Hard-core repulsion, a quantum effect, is needed to stabilize the lattice. In the simplified model of impenetrable hard spheres, the ions touch at the hard-sphere radius, and the lattice constant  $a$  of the cubic phase is twice the sum of the B and X ion radii. Pushing the X anions a distance  $u$  off the B-X-B axis by a tilt, the lattice constant changes to  $a + \delta a$  where  $\delta a = -2u^2/a$ . The Madelung energy per cell of the  $\text{B}^{3+}\text{X}_3^{-1}$  cubic lattice is  $U_M(V) = -17.908\beta^2 e^2 / V^{1/3}$  per cell, where  $V = a^3$  is the volume per cell. When  $V$  shifts to  $V + \delta V$ , where  $\delta V = a^2(\delta a_x + \delta a_y + \delta a_z)$ , the first order shift  $U_M(V + \delta V) - U_M(V)$  under a rigid tilt by  $u$  is thus  $-(1/2)\gamma_V \mu_D^2$  where  $\gamma_V = (4/3)17.908/a^3$  is the volume stabilization energy per dipole caused by the tilt  $u$ .

The induced moment is the one which minimizes this energy, giving

$$\mu_I / \mu_D = -(\gamma_M - \gamma_D) / (1/\alpha - \gamma_D). \quad (3)$$

For the parameters of  $\text{AlF}_3$ , this gives  $\mu_I \sim -0.80\mu_D$ . The total energy, evaluated at this optimal choice of in-

duced moment, is

$$U_{\text{tot}}(\mu_D, \mu_{I,\text{opt}}) = \frac{1}{2} \left( \gamma_M - \gamma_D - \gamma_V - \frac{(\gamma_M - \gamma_D)^2}{1/\alpha - \gamma_D} \right) \mu_D^2. \quad (4)$$

If we had not included the anion polarizability (*i.e.*  $\alpha \rightarrow 0$ ) then, for the parameters of  $\text{B}^{3+}\text{X}_3^{-1}$ , the net restoring coefficient  $\gamma_M - \gamma_D - \gamma_V$  would still be positive. In fact, our impenetrable sphere model probably overestimates  $\gamma_V$ , so stability is still fairly strong. However, there is a critical polarizability  $\alpha_c$  beyond which the quadratic restoring energy on dipoles goes negative, given by

$$\frac{1}{\alpha_c} = \gamma_D + \frac{(\gamma_M - \gamma_D)^2}{\gamma_M - \gamma_D - \gamma_V}. \quad (5)$$

For our simplified model of  $\text{AlF}_3$ , this is  $0.136\text{\AA}^3$ . Instability thus occurs even for  $\alpha$  well below the actual value for  $\text{F}^-$ ,  $\alpha \approx 0.85 \pm 0.05 \text{\AA}^3$  [12].

The theory presented here includes classical electrostatic energies quite well (since non-overlapping charge distributions interact to good approximation as if they were point charges and dipoles) but lumps all quantum effects into a hard core, possibly overstating the amount of energy available in volume contraction. Our theory omits all higher than quadratic effects and thus cannot predict the magnitude of the tilt. Nevertheless, we have offered a sensible approximation with no free parameters, which helps explain nicely the nearly universal instability of perovskite materials to octahedron tilting. Furthermore, the model predicts very little energy discrimination between different tilting schemes, consistent with the wide range of tilts seen experimentally (and sometimes adopted by the same material at different temperatures). The major influence of dipole-dipole interactions and anion polarizability are an interesting surprise.

## Acknowledgments

We thank P. E. Madden, M. Wilson, and V. Perebeinos for guidance in our earlier work which stimulated this paper. The work was supported in part by NSF grant no. DMR-0089492. PBA was supported in part by a J. S. Guggenheim Foundation fellowship. Work at Columbia was supported in part by the MRSEC Program of the NSF under award no. DMR-0213574. CPG thanks the Basic Energy Sciences program of the Department of Energy for support via grant no. DEFG0296ER14681.

## APPENDIX

A generalized CM theory [13] can be constructed as follows. For an array of point polarizable molecules at fixed positions  $\vec{R}_i$ , the energy for an arbitrary pattern of

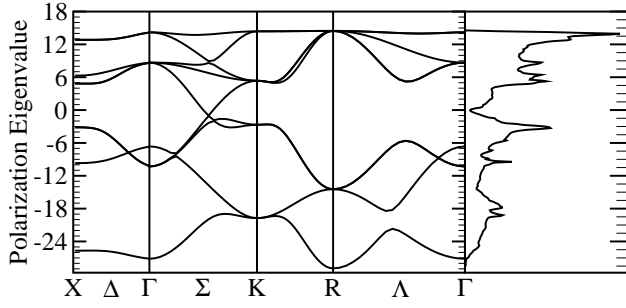


FIG. 3: Eigenvalues of the dipole-dipole interaction  $\Gamma$  versus wavevector for dipoles on the three  $F^-$  sublattices of the perovskite  $AlF_3$  structure. The largest eigenvalue is the five-fold degenerate state at the R point  $(\pi, \pi, \pi)$ , with eigenvalue 14.461. At the right, the density of states is plotted horizontally versus energy vertical.

dipoles  $\{\vec{\mu}_i\}$  is

$$\mathcal{E}(\{\vec{\mu}_i\}) = \sum_i \left( \frac{\mu_i^2}{2\alpha} - \frac{1}{2} \vec{\mu}_i \cdot \vec{F}_{D,i} \right) = \frac{1}{2} \langle \mu | \frac{1}{\alpha} \hat{1} - \Gamma | \mu \rangle. \quad (A.1)$$

For dipoles on the X anions in perovskite structure, there are 3 sublattice sites per cubic unit cell. A vector space notation is used where  $|\mu\rangle$  is a  $9N$ -dimensional column vector of the 3 Cartesian components of each of the  $3N$  dipoles in  $N$  unit cells, and  $\Gamma$  is the  $9N \times 9N$  dipole-dipole interaction matrix which has elements

$$\Gamma_{i\alpha,j\beta} = \frac{3R_{ij\alpha}R_{ij\beta} - \delta_{\alpha\beta}R_{ij}^2}{R_{ij}^5}. \quad (A.2)$$

The lattice is stable against dipole formation if the quadratic form Eq.(A.1) is positive (all its eigenvalues should be positive.) The condition for instability is that

the maximum eigenvalue  $\gamma$  of the matrix  $\Gamma$  exceeds the restoring force constant  $1/\alpha$ . The corresponding eigenvector gives the pattern of displacement dipoles  $|\mu\rangle$  which has the most self-stabilizing displacement pattern.

Bloch's theorem allows eigenstates of  $\Gamma$  to be chosen as simultaneous eigenstates of translations  $T(\vec{R})$  where  $\vec{R}$  is any translation vector of the primitive (simple cubic) lattice. The resulting Bloch states are labeled by wavevector  $\vec{k}$  which lies in the first Brillouin zone. The eigenvalues were computed numerically, using an Ewald method [14] to converge the sums. Results are shown in Fig. 3. As a test of the code, eigenvalues were also calculated for a model with a fourth sublattice corresponding to the perovskite A sites. Together with the three X sites, the resulting lattice is equivalent to the face-centered cubic structure in a non-primitive conventional cube and a four-atom basis. It was found numerically that the largest eigenvalue equalled  $4\pi n/3$  (with  $n = 4/a^3$ ) and occurred at  $\vec{k} = (000)$ . This is the known result of CM theory – when every molecule bears the same moment  $\vec{\mu}$  and sits on a site of cubic symmetry, the field at each site is given by the classical Lorentz value  $(4\pi/3)\vec{P}$ , and a ferroelectric instability occurs when the energy  $-\vec{P} \cdot \vec{F}$  exceeds the cost  $\mu^2/2\alpha$  to create the dipoles.

The flatness of the uppermost branch of  $\gamma$  versus  $k$  in Fig. 3 indicates that there is not much interaction coupling the  $xy$ -oriented dipoles in one  $xy$  plane to the  $xy$ -oriented dipoles in adjacent planes. This result can be understood as a consequence of the exponentially rapid transverse decay of electric field of a periodic array of dipoles [13]. This fact helps explain why the observed tilts of perovskites are so indiscriminating in their preferred wavevector  $(\pi, \pi, 0)$  *vs.*  $(\pi, \pi, \pi)$ , and even allow mixed wavevector solutions.

- 
- [1] J. C. Slater, Phys. Rev. **78**, 748 (1950).
  - [2] P. Daniel, A. Bulou, M. Rousseau, and J. Nouet, Phys. Rev. B **42** 10545 (1990).
  - [3] R. C. Shannon, Acta Cryst. **A32**, 751 (1976).
  - [4] J. D. Jackson, *Classical Electrodynamics*, 3rd Ed., Wiley, New York, 1999, pp 152-155.
  - [5] F. Jona and G. Shirane, *Ferroelectric Crystals*, Macmillan, New York, 1962.
  - [6] A. M. Glazer, Acta Cryst. B **28**, 3384 (1972).
  - [7] P. M. Woodward, Acta Cryst. B **53**, 32 and 44 (1997).
  - [8] Y.-R. Chen, P. B. Allen, and V. Perebeinos, Phys. Rev. B **69**, 054109 (2004).
  - [9] S. Chaudhuri, P. Chupas, M. Wilson, P. Madden, and C. P. Grey, J. Phys. Chem B **108**, 3437 (2004).
  - [10] M. E. Lines and A. M. Glass, *Principles and Applications of Ferroelectrics and Related Materials*, Clarendon Press, Oxford, 1977.
  - [11] W. Känzig, Solid State Physics **4**, 1 (1957).
  - [12] C. Kittel, *Introduction to Solid State Physics*, 6th Ed., Wiley, New York, 19xx, p.xxx.
  - [13] P. B. Allen, J. Chem. Phys. **120**, 2951 (2004).
  - [14] W. Smith, CCP5 Newsletter No. 46, Oct. 1998, p.18.